Table S1. Correlations between PDGFRβ and the mesenchymal signature in TNBC[a]

Upregulated genes (>2) in MES subtype			Downregulated genes (>2) in MES subtype		
gene	r[b]	p	gene	r	p
PCOLCE	0.826	1.3e-46	*MCM10*	-0.637	8.1e-22
ANPTL2	0.792	1.6e-40	*GINS1*	-0.637	1.2e-20
PRSS23	0.780	1.7e-38	*ATAD2*	-0.623	1.2e-20
SERPINF1	0.769	9.4e-37	*KIF11*	-0.618	2.9e-20
LRRC32	0.752	2.9e-34	*MCM4*	-0.618	3.0e-20
SRPX2	0.737	2.1e-32	*CDCA7*	-0.606	2.6e-19
FBN1	0.735	4.0e-32	*MELK*	-0.586	8.5e-18
SFRP4	0.731	1.3e-31	*CHEK1*	-0.577	3.6e-17
NDN	0.728	2.7e-31	*ESPL1*	-0.568	1.5e-16
CCDC80	0.724	8.0e-31	*KIF15*	-0.567	1.9e-16
ZNF423	0.716	7.2e-30	*RAD51AP1*	-0.559	6.8e-16
IGFBP4	0.715	8.8e-30	*FANCD2*	-0.559	6.6e-16
OLFML1	0.710	3.5e-29	*KIF14*	-0.557	9.0e-16
WISP2	0.709	4.9e-29	*RAD51*	-0.559	6.8e-16
LAMA4	0.709	5.4e-29	*FANCD2*	-0.559	6.6e-16
SEMA5A	0.707	7.8e-29	*KIF14*	-0.557	9.0e-16
CPXM1	0.703	2.2e-28	*DEPDC1B*	-0.556	9.7e-16
MRGPRF	0.699	6.8e-28	*BUB1*	-0.552	1.9e-15
PRRX1	0.696	1.4e-27	*CCNB1*	-0.552	1.7e-15
DCN	0.690	6.1e-27	*DTL*	-0.549	2.8e-15
FBLN1	0.687	1.4e-26	*EZH2*	-0.546	4.4e-15
SVEP1	0.687	1.3e-26	*NUF2*	-0.545	5.2e-15
SLIT3	0.684	2.6e-26	*PRC1*	-0.541	8.9e-15
LDB2	0.683	3.4e-26	*TTK*	-0.540	1.0e-14
FAM198B	0.674	3.4e-25	*BUB1B*	-0.539	1.2e-14
MN1	0.671	6.1e-25	*RACGAP1*	-0.538	1.4e-14
ROBO4	0.670	7.2e-25	*DLGAP5*	-0.537	1.52-14
SPON1	0.670	7.7e-25	*PBK*	-0.532	2.6e-14
CDH5	0.669	1.0e-24	*MCM2*	-0.533	2.6e-14
GNG11	0.666	2.0e-24	*UHRF1*	-0.532	3.0e-14
FMOD	0.661	5.9e-24	*NDC80*	-0.522	1.2e-13
RARRES2	0.660	7.1e-24	*HELLS*	-0.522	1.2e-13
COX7A1	0.659	9.5e-24	*CASC5*	-0.520	1.6e-13
LOX	0.658	1.1e-23	*ASPM*	-0.520	1.6e-13
HSPA12B	0.657	1.3e-23	*NCAPG*	-0.519	1.6e-13
CXCL12	0.657	1.2e-23	*KIF2C*	-0.513	3.6e-13
COL15A1	0.650	6.1e-23	*FAM83D*	-0.510	5.3e-13
ECM2	0.649	7.3e-23	*MTFR*	-0.508	6.7e-13
RUNX1T1	0.648	7.8e-23	*ECT2*	-0.506	9.1e-13
FSTL1	0.647	1.0e-22	*CENPK*	-0.506	9.4e-13
OMD	0.647	1.1e-22	*HMMR*	-0.505	1.1e-12
CPE	0.645	1.7e-22	*CENPF*	-0.505	1.0e-12
JAM2	0.645	1.6e-22	*AURKA*	-0.501	1.8e-12
SMOC2	0.644	1.8e-22	*RRM2*	-0.501	1.7e-12
EHD2	0.644	1.8e-22	*CDK1*	-0.498	2.6e-12

TNS1	0.641	3.5e-22	DHTKD1	-0.496	3.3e-12
DLC1	0.640	4.8e-22	CDCA8	-0.494	3.9e-12
IGFBP6	0.637	7.5e-22	TOP2A	-0.493	4.3e-12
DAB2	0.637	8.2e-22	LMNB2	-0.492	4.8e-12
MFAP4	0.635	1.2e-21	SPAG5	-0.490	6.6e-12
LIMA1	0.634	1.3e-21	CCNB2	-0.488	8.4e-12
RECK	0.634	1.5e-21	E2F8 TF	-0.488	8.5e-12
ZFPM2	0.633	1.7e-21	PTTG1	-0.488	8.2e-12
LHFP	0.633	1.7e-21	FOXM1 TF	-0.486 1	1.0e-11
MSRB3	0.632	2.2e-21	KIF4A	-0.485	1.2e-11
SLIT2	0.624	9.8e-21	NEK2	-0.485	1.1e-11
ERG	0.624	1.1e-20	CCNE2	-0.484	1.3e-11
HMCN1	0.623	1.2e-20	TYMS	-0.480	2.1e-11
LRRC17	0.623	1.2e-20	ZWINT	-0.478	2.5e-11
MAN1C1	0.622	1.4e-20	TRIP13	-0.477	2.8e-11
TIE1	0.622	1.3e-20	TPX2	-0.469	6.7e-11
AKAP12	0.622	1.4e-20	CCNA2	-0.468	7.7e-11
SPRY1	0.618	3.0e-20	ANLN	-0.467	8.9e-11
ACTA2	0.617	3.6e-20	IQGAP3	-0.466	9.4e-11
TGFBR2	0.616	4.3e-20	CDC7	-0.466	9.4e-11
MFAP5	0.615	5.7e-20	GTSE1	-0.465	1.1e-10
PECAM1	0.614	6.0e-20	BIRC5	-0.465	1.0e-10
VWF	0.614	6.3e-20	CEP55	-0.461	1.8e-10
CYBRD1	0.609	1.5e-19	KIF23	-0.458	2.4e-10
SCG2	0.602	5.6e-19	CDC20	-0.454	3.4e-10
ANTXR2	0.601	6.9e-19	CENPN	-0.454	3.3e-10
CFH	0.601	6.8e-19	E2F7 TF	-0.452	4.4e-10
F13A1	0.599	9.0e-19	RMI2	-0.446	8.3e-10
CPA3	0.596	1.7e-18	KIF20A	-0.442	1.2e-09
PDGFD	0.594	2.2e-18	CHMP4C	-0.437	1.9e-09
MYCT1	0.593	2.7e-18	CDCA2	-0.429	4.4e-09
CYGB	0.592	3.3e-18	CKS2	-0.428	4.8e-09
CD93	0.592	3.5e-18	KIAA0101	-0.425	6.8e-09
ADRA2A	0.591	3.8e-18	CXADR	-0.420	1.1e-08
DPT	0.590	4.3e-18	IL17RB	-0.419	1.2e-08
COL14A1	0.589	5.0e-18	CENPE	-0.414	1.8e-08
CLDN5	0.588	6.3e-18	GINS2	-0.410	2.6e-08
NNMT	0.587	7.7e-18	VANGL2	-0.403	4.9e-08
SPARCL1	0.585	1.1e-17	UBE2C	-0.403	4.9e-08
HSD17B11	0.584	1.1e-17	ESRP1	-0.395	9.6e-08
SYNPO2	0.580	2.4e-17	CENPA	-0.374	5.9e-07
HTR2B	0.579	2.7e-17	TK1	-0.371	7.5e-07
TWIST2	0.578	3.0e-17	HMGB3	-0.367	1.0e-06
PDPN	0.576	4.4e-17	CBX2	-0.364	1.2e-06
AGTR1	0.574	6.0e-17	SLC7A5	-0.360	1.6e-06
LAMA2	0.572	8.8e-17	CD24	-0.357	2.2e-06
CRTAP	0.571	9.9e-17	APOBEC3B	-0.335	1.0e-05
FMO1	0.571	9.5e-17	PABPC1L	-0.333	1.2e-05
VGLL3	0.570	1.2e-16	EPCAM	-0.333	1.2e-05

CAV1	0.569	1.3e-16	ZNF165 TF	-0.332	1.2e-05
FLRT2	0.567	1.8e-16	TFAP2A TF	-0.318	3.3e-05
PCSK5	0.566	2.1e-16	HN1	-0.314	4.0e-05
OGN	0.565	2.5e-16	OCLN	-0.310	5.4e-05
FHL1	0.565	2.5e-16			
PTPRB	0.565	2.4e-16			
LPAR1	0.564	2.8e-16			
CPED1	0.562	3.8e-16			
MEDAG	0.561	4.7e-16			
SOX17	0.558	6.9e-16			
GAS7	0.555	1.2e-15			
FEZ1	0.552	1.9e-15			
THBS4	0.551	2.2e-15			
PDE2A	0.550	2.3e-15			
TEK	0.550	2.3e-15			
EBF1	0.549	2.7e-15			
DUSP1	0.549	2.7e-15			
TCF4	0.547	3.5e-15			
IGF1	0.547	3.9e-15			
PHLDB2	0.546	4.0e-15			
PROS1	0.544	5.8e-15			
RBMS3	0.543	6.3e-15			
S1PR1	0.543	6.4e-15			
NOSTRIN	0.540	1.0e-14			
PAMR1	0.538	1.4e-14			
EPAS1	0.538	1.3e-14			
EMCN	0.538	1.4e-14			
ENPEP	0.536	1.7e-14			
RGS5	0.535	2.0e-14			
THBD	0.534	2.3e-14			
FZD4	0.533	2.5e-14			
FERMT2	0.532	3.1e-14			
PROCR	0.527	5.6e-14			
IL1R1	0.526	7.0e-14			
COLEC12	0.525	7.7e-14			
CST3	0.523	1.0e-13			
CES1	0.517	2.2e-13			
ABI3BP	0.511	4.9e-13			
MAF	0.509	6.4e-13			
ZEB2	0.508	7.5e-13			
SLC40A1	0.507	8.6e-13			
DUSP6	0.507	8.5e-13			
SNAI2	0.506	9.0e-13			
PDE7B	0.506	9.3e-13			
ITIH5	0.504	1.2e-12			
RHOJ	0.504	1.2e-12			
SCN4B	0.504	1.1e-12			
CFD	0.503	1.3e-12			
RNASE4	0.500	2.0e-12			

SEMA3	0.497	2.9e-12			
MEOX2	0.497	2.6e-12			
IL6ST	0.495	3.6e-12			
ABLIM3	0.495	3.3e-12			
CORO2B	0.493	4.7e-12			
MGLL	0.493	4.4e-12			
CXCL14	0.492	4.8e-12			
GEM	0.492	5.3e-12			
MAN1A1	0.487	9.1e-12			
CFI	0.486	1.0e-11			
FOLR2	0.486	1.0e-11			
PLSCR4	0.485	1.1e-11			
GPX3	0.481	1.8e-11			
CYP2U1	0.477	2.7e-11			
AQP1	0.475	3.8e-11			
GSTM5	0.474	3.8e-11			
TMEM140	0.474	4.2e-11			
ANK2	0.473	4.4e-11			
ADAMTS15	0.472	4.9e-11			
THSD7A	0.468	7.9e-11			
DCLK1	0.468	7.6e-11			
STEAP4	0.467	8.3e-11			
RNASE1	0.462	1.6e-10			
MYH11	0.461	1.7e-10			
GPC3	0.459	2.1e-10			
ADAMTS5	0.458	2.4e-10			
PLTP	0.457	2.5e-10			
TFPI	0.457	2.6e-10			
ARHGAP20	0.457	2.6e-10			
PPARG	0.456	2.8e-10			
FN1	0.456	2.7e-10			
FOS	0.455	3.1e-10			
INMT	0.453	4.0e-10			
KLF9	0.452	4.1e-10			
GPR146	0.452	4.2e-10			
SDPR	0.451	4.6e-10			
LPAR6	0.449	5.8e-10			
SEMA3C	0.446	7.9e-10			
CAV2	0.446	7.8e-10			
MFNG	0.446	7.8e-10			
PCDH18	0.444	1.0e-09			
AOX1	0.443	1.0e-09			
MME	0.440	1.5e-09			
PTGER3	0.440	1.5e-09			
FOXO1	0.440	1.5e-09			
CH25H	0.438	1.7e-09			
GIMAP6	0.438	1.8e-09			
MAMDC2	0.436	2.3e-09			
VIM	0.433	3.0e-09			

A2M	0.431	3.6e-09			
LYVE1	0.431	3.7e-09			
PDK4	0.429	4.4e-09			
MECOM	0.428	4.8e-09			
CD36	0.426	5.9e-09			
LY96	0.421	9.5e-09			
KCTD12	0.419	1.1e-08			
CLDN11	0.416	1.5e-08			
CDO1	0.415	1.6e-08			
ZBTB16	0.415	1.7e-08			
PLIN4	0.414	1.8e-08			
KCND3	0.414	1.8e-08			
FOSB	0.412	2.2e-08			
C7	0.412	2.2e-08			
AKR1C3	0.411	2.5e-08			
DIXDC1	0.411	2.3e-08			
ATP1A2	0.410	2.6e-08			
FABP4	0.409	2.8e-08			
CD209	0.408	3.2e-08			
SELP	0.407	3.5e-08			
P2RY14	0.407	3.5e-08			
NOVA1	0.406	3.7e-08			
RGL1	0.406	3.8e-08			
MSR1	0.405	4.1e-08			
CR1	0.401	6.0e-08			
PALMD	0.400	6.2e-08			
ALDH1A2	0.400	6.2e-08			
C10orf10	0.399	7.2e-08			
DNASE1L3	0.397	8.0e-08			
STEAP2	0.397	8.2e-08			
DDR2	0.395	9.8e-08			
ADIPOQ	0.395	9.6e-08			
TMEM176B	0.394	1.1e-07			
PIK3R1	0.393	1.1e-07			
FBLN5	0.393	1.2e-07			
ENPP2	0.391	1.5e-07			
FLI1 TF	0.391	1.3e-07			
TIMP4	0.390	1.5e-07			
GIMAP1	0.390	1.5e-07			
PTGIS	0.390	1.5e-07			
SORBS1	0.388	1.7e-07			
VSIG4	0.384	2.6e-07			
CHL1	0.383	2.6e-07			
MS4A4A	0.383	2.8e-07			
HBB	0.383	2.8e-07			
SEPP1	0.383	2.7e-07			
HAS2	0.382	2.9e-07			
SLC16A7	0.382	3.0e-07			
CD14	0.381	3.2e-07			

ANXA1	0.377	4.4e-07			
CIDEC	0.376	5.0e-07			
TNN	0.376	4.8e-07			
G0S2	0.375	5.1e-07			
SOX7	0.373	6.1e-07			
PLIN1	0.372	6.5e-07			
ADH1B	0.369	8.3e-07			
APOLD1	0.369	8.4e-07			
ADAMTS18	0.367	1.0e-06			
STEAP1	0.367	9.9e-07			
MEF2C TF	0.366	1.1e-06			
ITM2A	0.363	1.4e-06			
MEOX1 TF	0.362	1.4e-06			
MPEG1	0.361	1.6e-06			
SOCS2	0.361	1.6e-06			
PTGDS	0.359	1.8e-06			
TSPAN7	0.354	2.6e-06			
MAOA	0.353	2.9e-06			
SLC2A3	0.353	2.8e-06			
GLDN	0.352	3.1e-06			
PLA2G16	0.352	3.1e-06			
THRB TF	0.350	3.6e-06			
GPAM	0.349	3.9e-06			
ACSL1	0.348	4.1e-06			
PLA2G2A	0.347	4.5e-06			
ABCA6	0.345	5.0e-06			
NRN1	0.343	5.9e-06			
CLN5	0.342	6.3e-06			
GHR	0.341	6.9e-06			
THRSP	0.340	7.3e-06			
BMPER	0.340	7.5e-06			

[a] All the genes belong to the mesenchymal signature as described by Burstein et al. [6].
[b] Correlations were analyzed by χ^2 Pearson's test through the R2 platform [28].

A

B

C
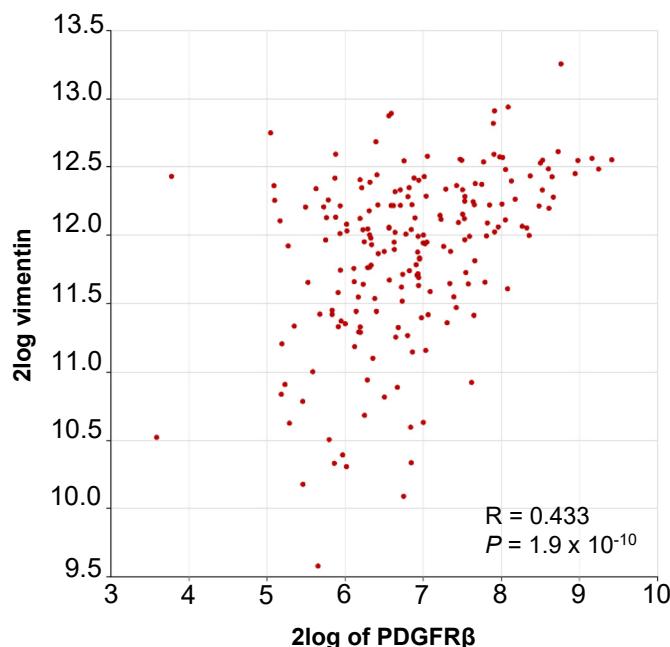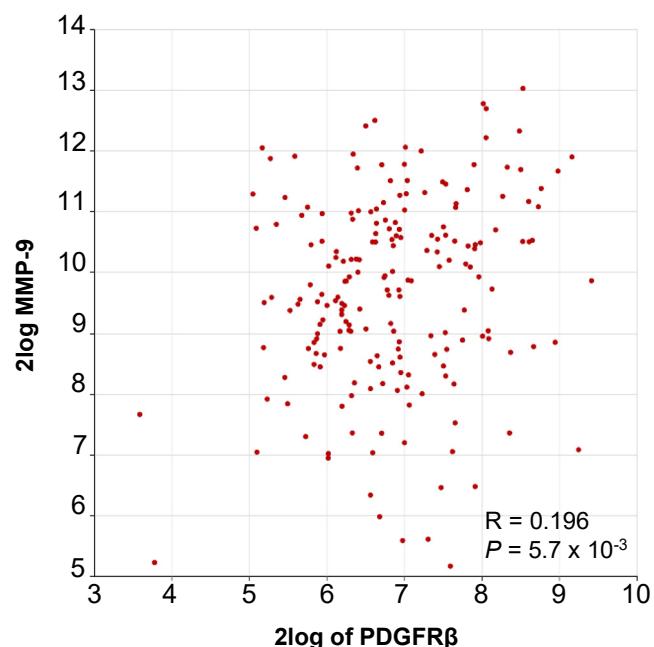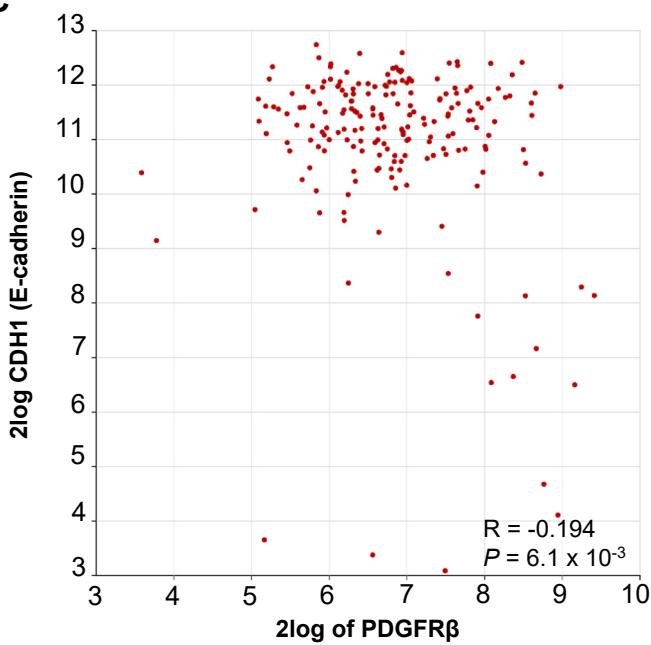
Figure S1. PDGFRβ gene correlations in human TNBC tissues. (**A-C**) XY-blots correlating PDGFRβ gene with vimentin (**A**), MMP-9 (**B**) and CDH1/E-cadherin (**C**) genes in TNBC tissues (GSE76124). Correlations were analyzed by the Pearson's χ^2 test through the R2 platform [28]. Significance of correlation was assessed by r-value (R) and p-value (*P*). MMP-9: matrix metallopeptidase-9; PDGFRβ: platelet-derived growth factor receptor β.
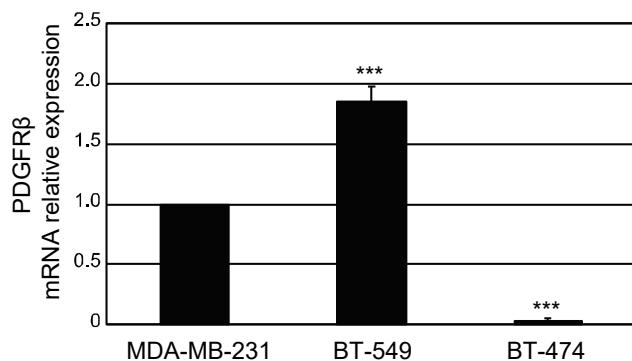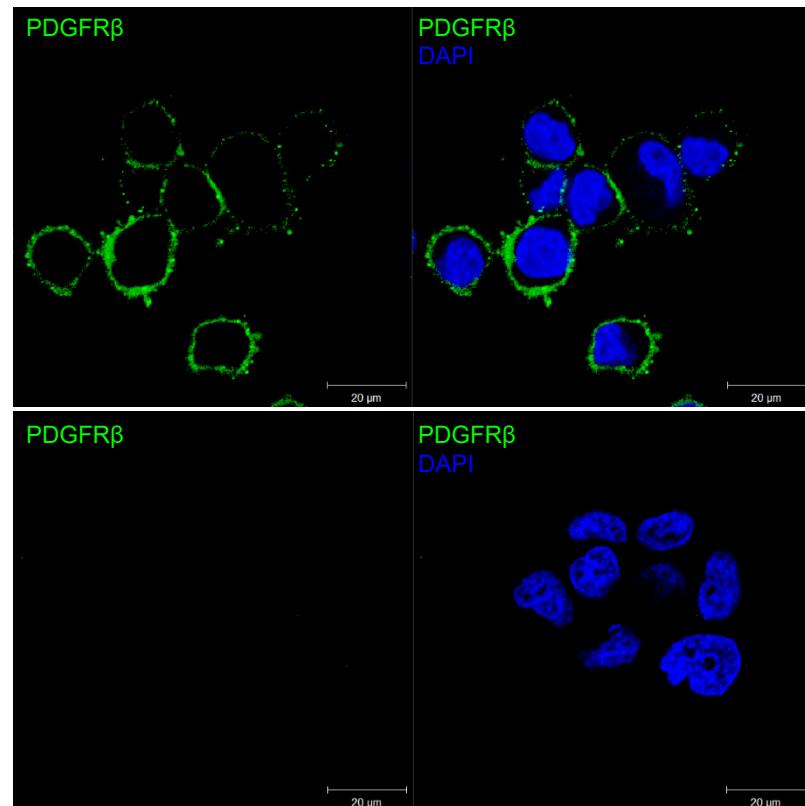
Figure S2. PDGFRβ expression in mesenchymal TNBC MDA-MB-231 and BT-549 cells. (**A**) PDGFRβ mRNA expression in TNBC MDA-MB-231 and BT-549 cells was analyzed by RT-qPCR. HER2-positive and PDGFRβ-negative breast cancer BT-474 cells were used as negative control [30]. Bars depict means ± SD of three independent experiments. ***$P < 0.001$ relative to MDA-MB-231 cells. (**B**) MDA-MB-231 and BT-474 cells were fixed and labeled with anti-PDGFRβ antibody without permeabilization, visualized by confocal microscopy and photographed. PDGFRβ and nuclei are visualized in green and blue, respectively. All digital images were captured at the same setting to allow direct comparison of staining patterns. Magnification 63 ×, scale bar = 20 μm. DAPI: 4′,6-Diamidino-2-phenylindole; PDGFRβ: platelet-derived growth factor receptor β.
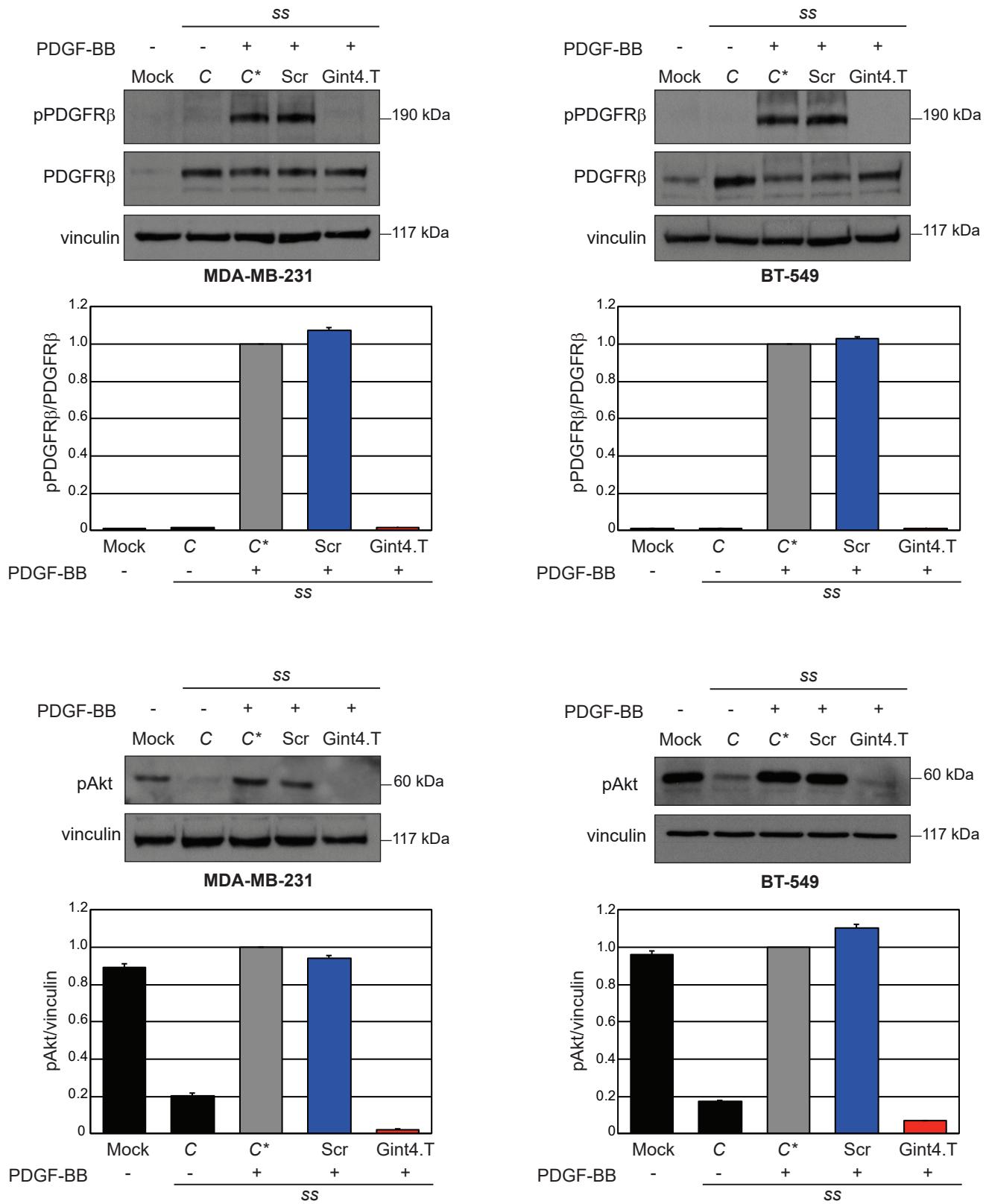
Figure S3. PDGFRβ aptamer inhibits PDGF-BB-dependent PDGFRβ activation in mesenchymal TNBC cells. MDA-MB-231 and BT-549 cells (2×10^5) were serum-starved for 18 h (*ss*) and then left untreated (*C*) or stimulated for 10 min with 100 ng/mL PDGF-BB in the absence (*C**) or in the presence of 200 nM anti-PDGFRβ (Gint4.T) or scrambled negative control (Scr) aptamer, as indicated. Cell lysates were immunoblotted with anti - pPDGFRβ and anti-pAkt antibodies. Filters were stripped and reprobed with anti - PDGFRβ antibody, as indicated. Equal loading was confirmed by immunoblot with anti - vinculin antibody. Molecular weights of indicated proteins are reported. Depicted results represent one of three typical experiments performed. The histograms indicate pPDGFRβ/PDGFRβ and pAKT/vinculin ratio of densitometric signals, reported as relative to cells stimulated in the absence of aptamer (*C**), arbitrarily set to 1. Bars depict means ± SD of three independent experiments. PDGFRβ: platelet-derived growth factor receptor β; PDGF-BB: platelet derived growth factor-BB.
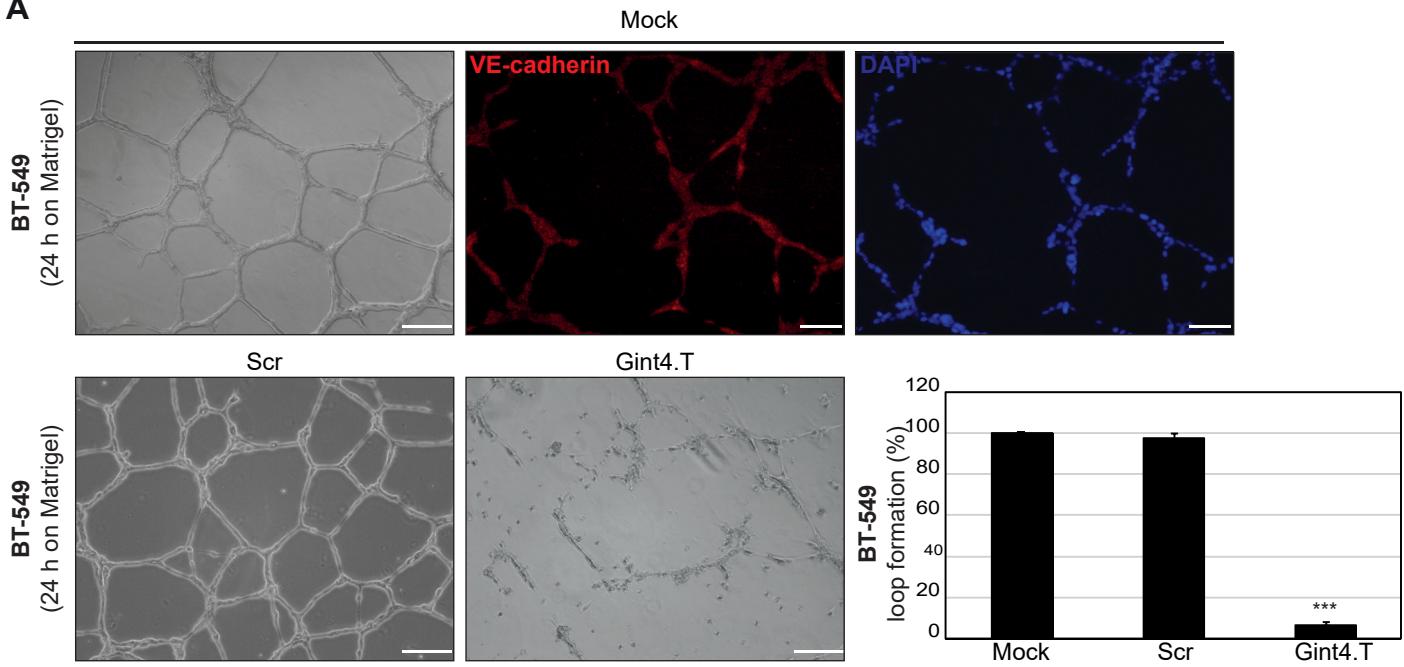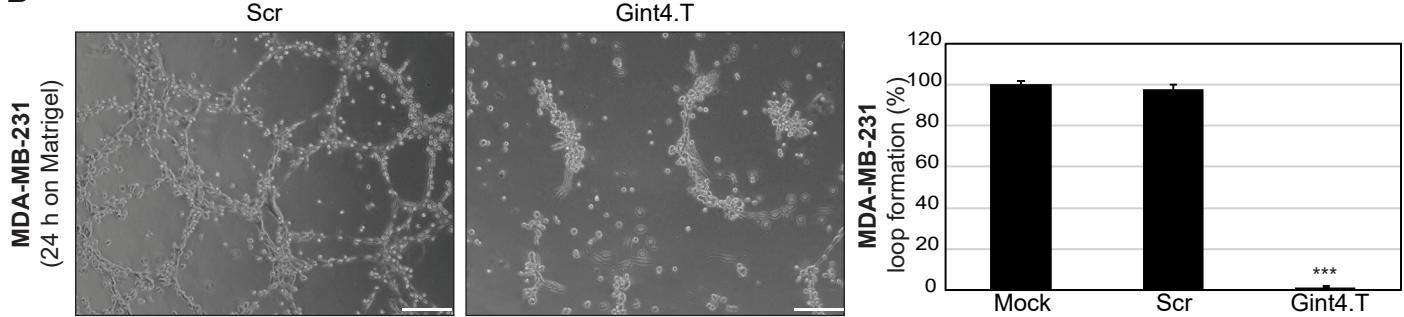
Figure S4. PDGFRβ aptamer inhibits tube formation ability of mesenchymal TNBC cells. (**A**) BT-549 and (**B**) MDA-MB-231 cells were seeded on Matrigel monolayer in the absence (Mock) or in the presence of 200 nM Gint4.T or Scr for 24 h. Cells were photographed by phase-contrast microscopy. Magnification 10 ×, scale bar = 200 μm. (**A-B**) Tube formation ability was determined as the percentage of reduction in loop formation of treated cells compared with mock-treated cells. Bars depict means ± SD of three independent experiments. ***$P < 0.001$ relative to mock. (**A**) BT-549 cells, seeded on Matrigel for 24 h, were stained with anti-VE-cadherin antibody, visualized by fluorescence microscopy and photographed; nuclei were stained with DAPI. Magnification 20×, scale bar = 100 μm. DAPI: 4′,6-Diamidino-2-phenylindole; VE: vascular endothelial.
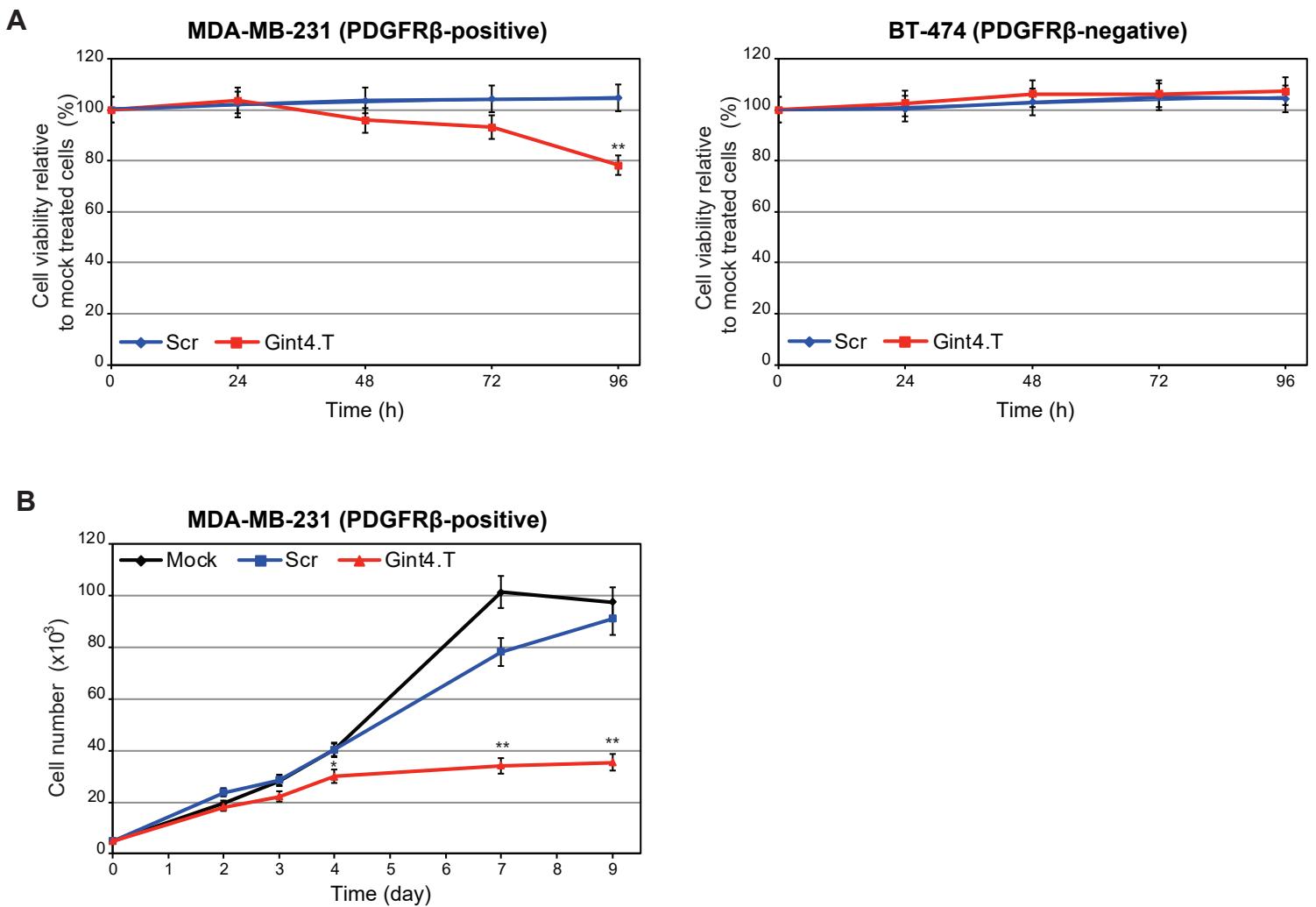
**Figure S5. Inhibition of MDA-MB-231 cell proliferation after a prolonged Gint4.T treatment**. (**A**) Viability of MDA-MB-231 (PDGFRβ-positive) and BT-474 (PDGFRβ-negative) cells mock-treated or treated with 200 nM Gint4.T or Scr for the indicated incubation times. Data are expressed as percent of viable treated cells with respect to mock-treated cells. (**B**) Growth curves of MDA-MB-231 cells mock-treated or treated with 200 nM Gint4.T or Scr for the indicated incubation times. (**A-B**) The aptamer treatment was renewed each 24 h. Bars depict means ± SD of three independent experiments. **$P < 0.01$; *$P < 0.05$. PDGFRβ: platelet-derived growth factor receptor β.

A

NH2-Scr
NH2-Gint4.T   VivoTag-S 680

5'NH2 + NIR → NIR

NIR-Scr   NIR-Gint4.T

1.70
1.27
0.85
0.43
0.00
[Count/Energy]

B

x10³

11863.2827

Intensity [a.u.]

Count vs.
Deconvoluted Mass (amu)
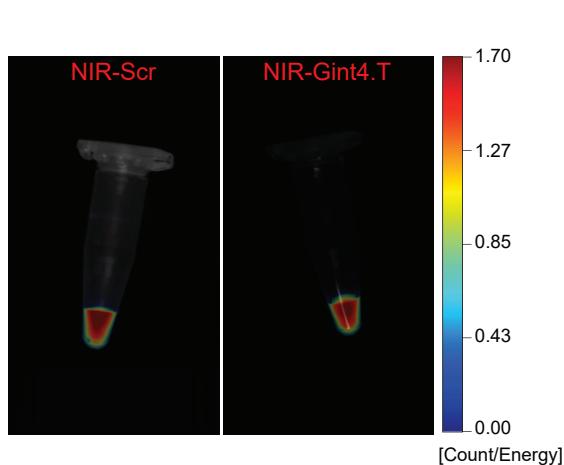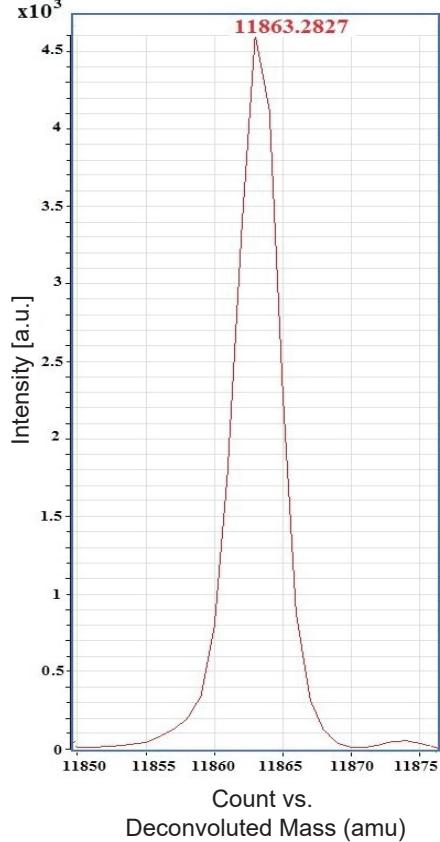
ESITOF-MS (M+H$^+$)	m/z (Da)
found	11863
expected	11862

Figure S6. NIR-labeling of RNA aptamers. (**A**) Amino-terminated Gint4.T and Scr aptamers were labeled with VivoTag-S 680 NIR-dye and imaged by 2D FMT analysis (shown are representative images from 1000 pmol aptamers). (**B**) ESITOF mass spectrum of NIR-Gint4.T: m/z value relative to M+H$^+$. ESITOF-MS: m/z calculated for M+H$^+$ = 11862 Da; m/z found: 11863 Da.   ESI: electron spray ionization; MS: mass spectrometry; NIR: near-infrared; TOF: time-of-flight.
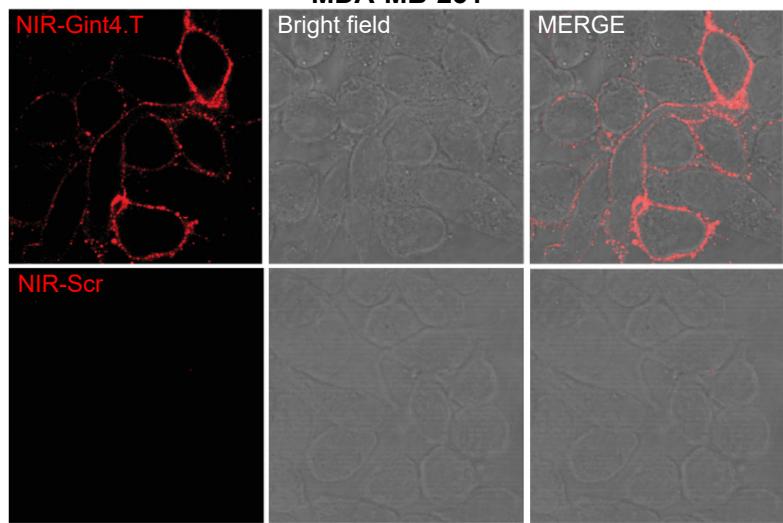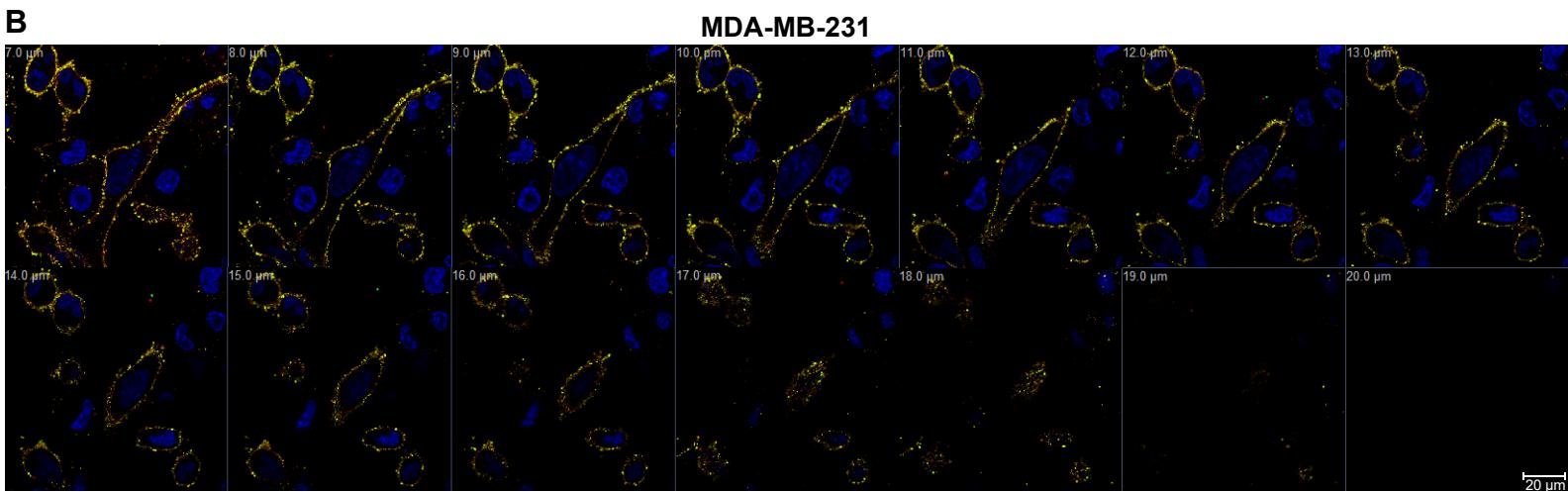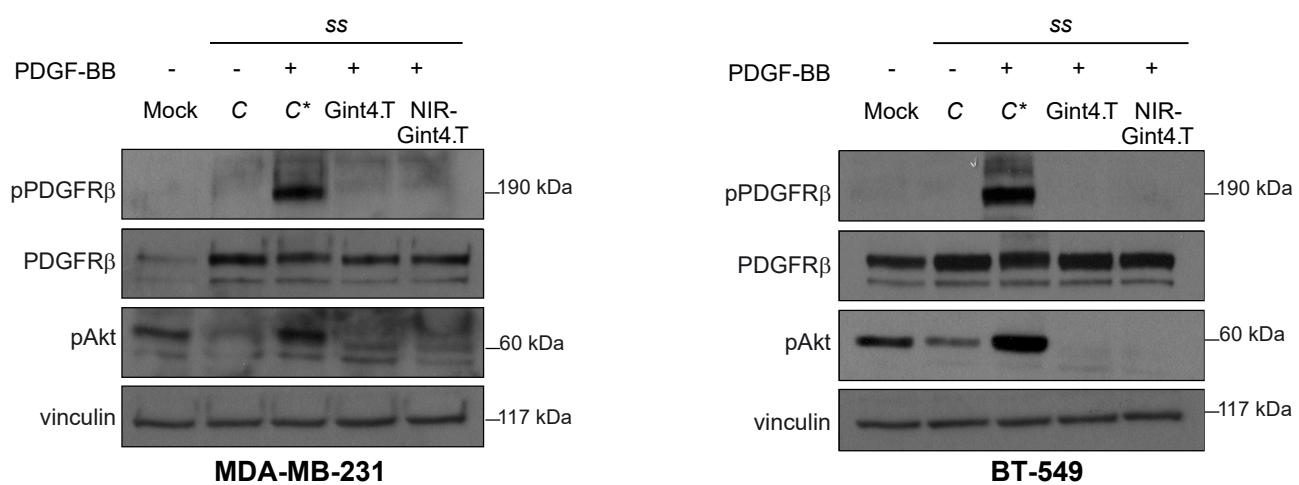
Figure S7. NIR-Gint4.T binds to PDGFRβ and inhibits its activation in TNBC cells. (**A**) Representative confocal images (fluorescence, bright field, merge) of MDA-MB-231 cells incubated for 5 min with 500 nM NIR-Gint4.T or NIR-Scr. (**B**) Following 5 min incubation with 500 nM NIR-Gint4.T, MDA-MB-231 cells were fixed and labeled with anti-PDGFRβ antibody without permeabilization. Z-scan images collected at 1.0 μm sections are shown. NIR-Gint4.T, PDGFRβ and nuclei are visualized in red, green and blue, respectively. Co-localization results appear yellow in the merged images. (**A-B**) All digital images were captured at the same setting to allow direct comparison of staining patterns. (**A**) Magnification 63 ×, 2.0 × digital zoom. (**B**) Magnification 63 ×, scale bar = 20 μm. (**C**) MDA-MB-231 and BT-549 cells were serum-starved (*ss*) and then left untreated (*C*) or stimulated with PDGF-BB in the absence (*C**) or in the presence of Gint4.T or NIR-Gint4.T, as reported in the legend to Figure S3. Depicted results represent one of three typical experiments performed. NIR: near-infrared; PDGFRβ: platelet-derived growth factor receptor β; PDGF-BB: platelet derived growth factor-BB.
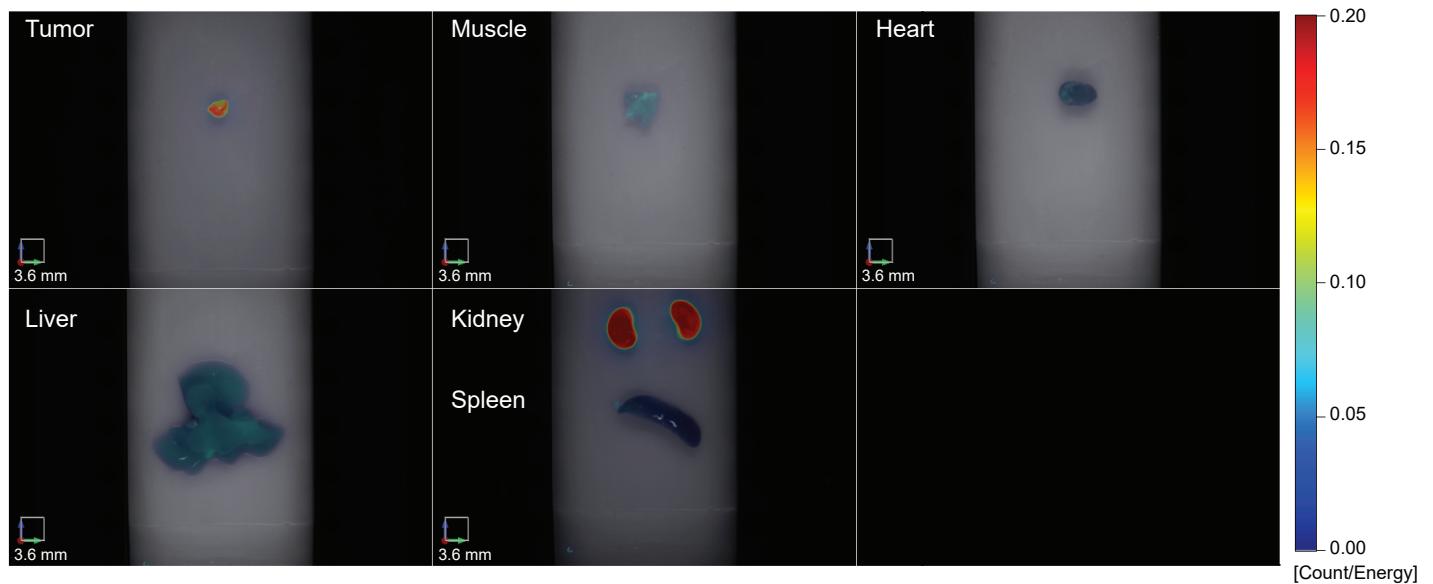
Figure S8. *Ex vivo* FMT imaging analysis. Representative 2D FMT imaging of tumor and major organs (muscle, heart, liver, spleen and kidney) harvested from mice bearing *s.c.* MDA-MB-231 tumors at 24 h post-injection of NIR-Gint4.T.
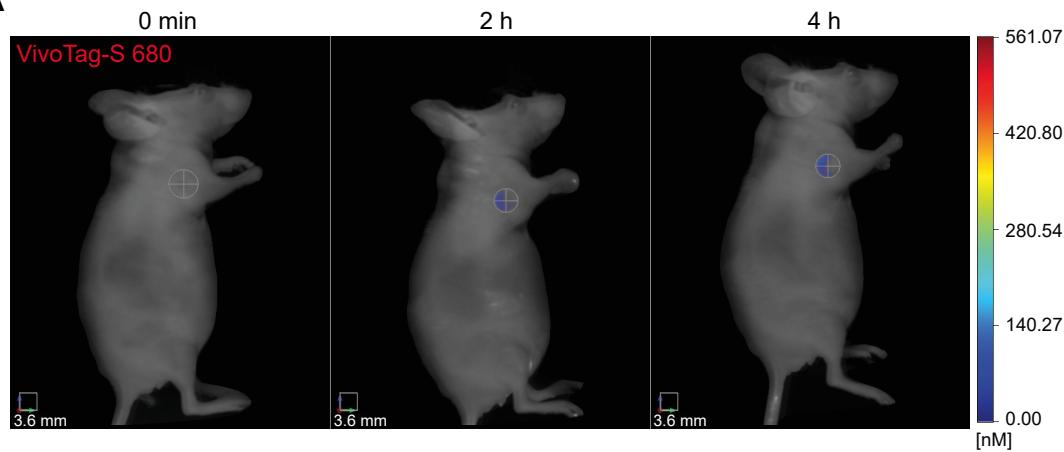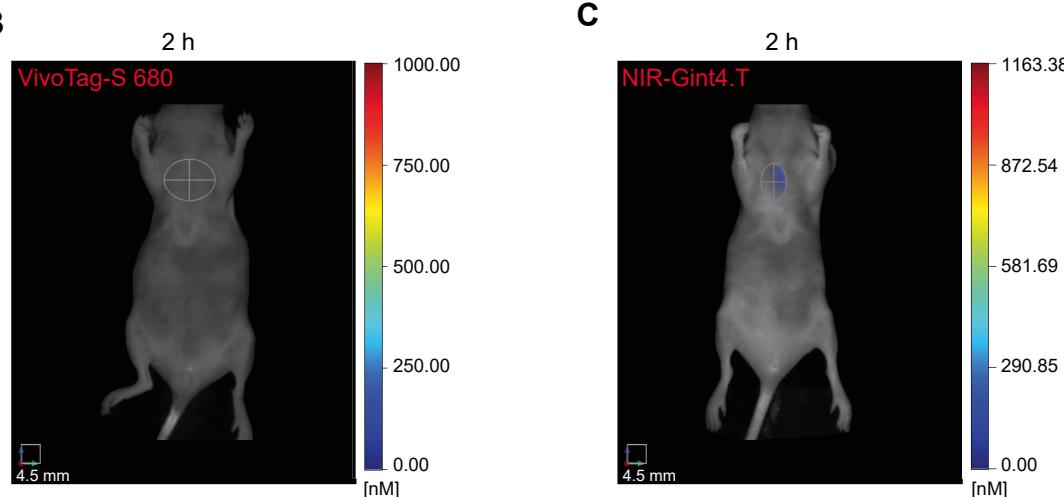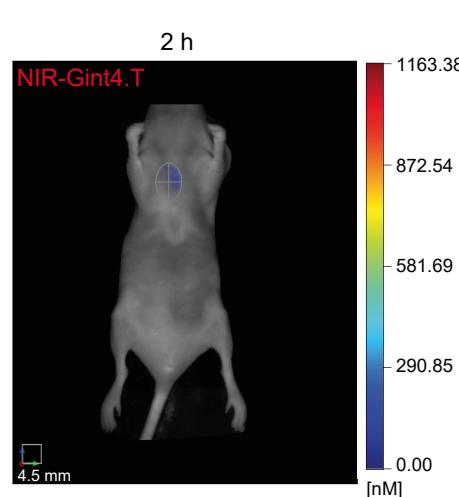
Figure S9. Negative controls for nonspecific NIR detection *in vivo*. Representative *in vivo* imaging of mice bearing *s.c.* MDA-MB-231 tumors (**A**) or MDA-MB-231-derived lung metastases (**B**) after *i.v.* injection of 1 nmol VivoTag-S 680. No signal was revealed with VivoTag-S 680 alone. (**C**) Representative *in vivo* imaging of healthy mice *i.v.* injected with 1 nmol NIR-Gint4.T. (**A-C**) All *in vivo* imaging control analyses were performed contextually to imaging by NIR-Gint4.T. NIR: near-infrared.
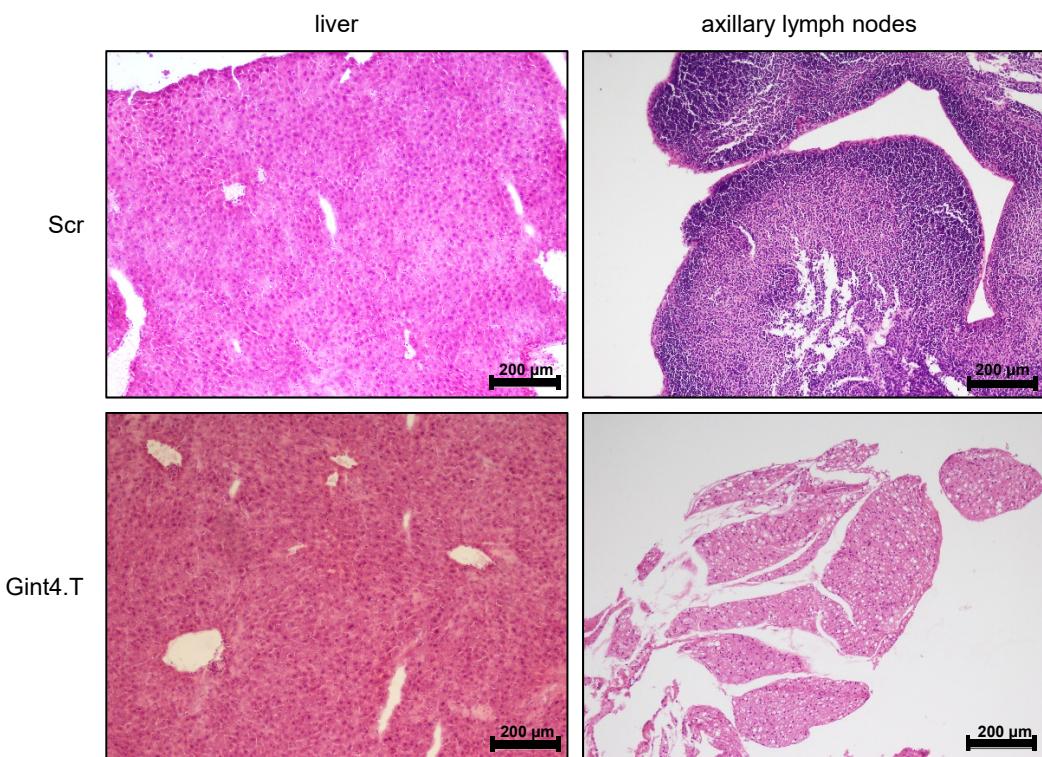
Figure S10. Blockade of lung metastasis by Gint4.T does not cause a relocation of metastasis. Representative H&E staining of liver and axillary lymph nodes harvested from Gint4.T- and Scr-treated mice. Magnification 10 ×, scale bar = 200 μm.